Journal of Orthopaedic Trauma
Vol. 16, No. 2, pp. 87–91

Biomechanical Consequences of Secondary Congruence After Both-column Acetabular Fracture

*Richard G. Levine, †Regis Renard, †Fred F. Behrens, and ‡Paul Tornetta III

**Department of Orthopaedics, Union Memorial Hospital, Baltimore, Maryland, U.S.A.; †Department of Orthopaedics, University of Medicine and Dentistry of New Jersey-New Jersey Medical School, Newark, New Jersey, U.S.A.; and ‡Department of Orthopaedics, Boston Medical Center, Boston, Massachusetts, U.S.A.*

Objectives: To create a both-column acetabular fracture model with secondary congruence and to determine the intraarticular loading characteristics present in simulated single-leg stance.
Hypothesis: The normal contact pressures on the weight-bearing portion of the acetabulum in simulated single-leg stance are different from those present in a both-column fracture model exhibiting secondary congruence.
Design: Cadaveric Biomechanical model.
Setting: Biomechanical testing laboratory.
Specimens: Nine fresh frozen cadaveric hemipelves.
Intervention: Both-column fracture model with secondary congruence of the acetabular articular surface with respect to the femoral head was created and tested using Materials Testing Machine (MTS Systems Corp., Minneapolis, MN) and Fuji pressure-sensitive film (Sensor Products, Inc., East Hanover, NJ).
Outcome Measurements: Testing data recorded and analyzed comparing the fractured and unfractured states.
Results: With respect to the intact specimen, the contact area, mean pressure, and peak pressure in the dome region all increased ($p < 0.003$) in the both-column model. The contact area in the anterior articular region decreased ($p < 0.02$) as did the mean pressure ($p < 0.032$). The posterior articular region demonstrated a trend toward decreased contact area and increased mean and peak pressures. Descriptively, the stress concentration shifted toward the fracture in all cases with the most anterior and most posterior articular regions having little contact in the fracture model.
Conclusions: In the authors' both-column model of secondary congruence, the stress concentration during simulated single-leg stance was increased significantly in the dome of the acetabulum adjacent to the fracture line.
Key Words: Acetabular fracture, Secondary congruence, Hip mechanics.

Clinical results after acetabular fractures are related to the congruence of the hip joint and the status of the roof (dome) (4,7–11,15,17). As in other joints, articular malreduction results in increased wear on the articular cartilage and subsequent posttraumatic arthritis. Because both the anterior and posterior columns are separated from the intact ilium, both-column fractures allow for "secondary congruence" of the joint. The columns rotate away from each other, allowing the articular surface to remain relatively congruent with the femoral head. The long-term results after nonoperative management of both-column fractures is better than other fracture patterns that affect the weight-bearing surface of the acetabulum (7,8,17). The purpose of this study was to determine the changes in the loading pattern in a cadaveric both-column fracture model that simulates union with secondary congruence.

MATERIALS AND METHODS

Seven fresh frozen cadaveric pelves and their respective femora were harvested (average age, seventy years). Before testing, two specimens with macroscopic arthritic changes were excluded. Prior to data collection, these specimens were used to test the stability of the pelvic model. All specimens were kept moist with normal saline. The pelves were cleaned of soft tissues, leaving the hip joint capsule intact. The pelves were then cut into nine hemipelves in the midsagittal plane, and potted via the sacroiliac joints in poly-methylmethacrylate. Two wood screws were used to reinforce the sacroiliac joints because this was the area of construct failure noted in the pretesting specimens. The poly-methylmethacrylate block was held in a vice with three degrees of freedom and the symphyseal body was stabilized with a bolt connected to the mounting construct. Each hemipelvis was mounted on a servo-hydraulic mechanical testing system

Accepted February 28, 2001.
Address correspondence and reprint requests to Richard G. Levine, M.D., Department of Orthopaedics, Union Memorial Hospital, 201 East University Parkway, Baltimore, MD 21218-2895, U.S.A.
The study was in part funded by an AO North America Resident Clinical Trauma Research Support Grant.

(MTS Systems Corporation, Minneapolis, MN) with the anterior superior iliac spine and the pubic tubercle aligned vertically and the plane of the ischial tuberosities parallel to the floor to reproduce pelvic alignment in the erect anatomic position. The model was then rotated twenty-five degrees internally in the coronal plane to simulate the joint reaction force vector in single-leg stance. The femur was potted with poly-methyl-methacrylate in the position of single leg stance (fifteen degrees adduction, zero degrees flexion, five degrees internal rotation) relative to the hemipelvis while on the MTS machine. Rotation of the femur was based on neutral position defined by placing the linea aspera in a directly posterior position. The joint capsule was removed leaving the labrum and transverse acetabular ligament intact. To reduce articular creep, each specimen was preloaded to 500 Newtons of compression at twenty millimeters/minute for five minutes. Fuji low-grade pressure-sensitive film (Sensor Products, Inc., East Hanover, NJ) (range, 2.5 to ten megapascals) was cut to a computer-generated saw tooth pattern designed to conform to a sphere. The film was applied to the femoral head which was covered with a latex condom (Trojan Latex Condom, Carter Wallace, New York, NY) and held in place with spray adhesive (Fig. 1). As described by Konrath et al., a second latex condom with a reported thickness of 250 micrometers was then placed over the film and femoral head. Each intact specimen was loaded to 1500 Newtons at a rate of twenty millimeters/minute to obtain baseline pressure data with the rim and the acetabular margins marked as reference points. A both-column fracture (OTA type 62–C1.1) was then constructed by creating an intermediate anterior column fracture with a coping saw cut to within three millimeters of subchondral bone and then fracturing the articular surface by levering open the fracture with an osteotome. The anterior column fracture was then externally rotated allowing a five-millimeter shim to be placed between the columns at the level of the joint while perfect congruence with the femoral head was maintained. Thus, the fracture had a five-millimeter gap between the anterior and posterior columns but no stepoff. The fracture was fixed in this position with standard reconstruction plates and position screws (Synthes USA, Paoli, PA, U.S.A.). The posterior column, which was fixed to the anterior column in the supra-acetabular region was then cut from the intact ilium through the greater sciatic notch and fixed to the ilium with reconstruction plates (Fig. 2). Thus, a model of secondary congruence was created as both the anterior and posterior joint surfaces were anatomically reduced to the femoral head but displaced five millimeters from one another. This construct was tested in the same manner as the intact specimen using pressure-sensitive film with the femur rotated externally five degrees (resulting in 14.88 degrees of adduction, 6.48 degrees of flexion, and five degrees of internal rotation relative to the pelvis) to simulate equal displacement of both the anterior and posterior columns from the perspective of the femoral head. All hips were loaded twice for each condition.

FIG. 1. Femoral head with Fuji pressure-sensitive film.

FIG. 2. Hemipelvis both-column fracture model.

The film was digitized using a flatbed scanner (Scanjet Plus, Hewlett Packard, Palo Alto, CA, U.S.A.) to a Power Macintosh 7100 (Apple Computer, Cupertino, CA, U.S.A.) for analysis using NIH Image 1.57 software (National Institute of Health, Bethesda, MD, U.S.A.). To filter the images, the background was first subtracted, followed by a smoothing process. The image was divided into anterior, dome, and posterior thirds for analysis (1). The optical densities and areas were measured in two-millimeter by two-millimeter square segments. The contact pressures were calculated using a previously made calibration curve and their optical densities. To create the calibration curve, the latex-film-latex construct was placed between two twenty-five millimeter diameter polyethylene cylinders. A series of loads were applied to the construct under a measured compressive pressure from one Mega Pascal to eleven Mega Pascal. The film was digitized and analyzed. Pressure versus optical stain density was plotted and a polynomial curve fitted to the points.

A repeated measures ANOVA with Fisher's protected least significant difference was performed using SuperANOVA software (Abacus Concepts Inc., Berkeley, CA, U.S.A.).

RESULTS

Nine hemipelvic specimens were tested. The contact pressure and pressure distribution for each hip joint was analyzed. The acetabulum was divided into three regions of equal size: anterior, dome, and posterior. For each region in the both-column model, the contact area, mean pressure, and peak pressures were recorded and compared with the intact specimen.

With respect to the intact specimen, the contact area, mean pressure, and peak pressure in the dome region all increased ($p < 0.003$) in the both-column model. The contact area in the anterior articular region decreased ($p < 0.02$) as did the mean pressure ($p < 0.032$). The posterior articular region demonstrated a trend toward decreased contact area and increased mean and peak pressures. These changes are summarized in Table 1 and Figs. 3–5. Descriptively, the stress concentration shifted towards the fracture in all cases with the most anterior and most posterior articular regions having little contact in the fracture model. The highest pressures were seen in the dome region with the both-column model manifesting 122 percent of the mean pressure and 280 percent of the peak pressure of the intact specimen.

TABLE 1. *Summary of data intact and both-column fractured (BC) specimens with respect to contact area, mean, and peak pressures**

	Anterior		Dome		Posterior	
Variable	Intact	BC	Intact	BC	Intact	BC
Area (%)	*30*	*18*	*37*	*55*	33	28
Mean pressure (MPa)	*1.9*	*1.6*	*1.8*	*2.2*	1.9	2.0
Peak pressure (MPa)	2.6	2.1	*2.3*	*6.5*	2.8	4.0

*Italic numbers are statistically significant to $p < 0.05$.

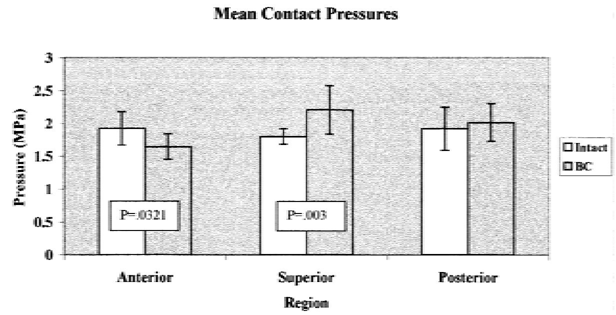

FIG. 3. Mean contact pressures for the intact and both-column models. This figure indicates the mean contact pressures (MPa) with one standard deviation within the anterior, superior, and posterior articular regions for the intact (n = 9) and both-column (n = 9) models.

DISCUSSION

Traditionally, the treatment of acetabular fractures is based on the assumption that anatomic restoration of the articular surface is necessary to avoid post-traumatic osteoarthritis and thus obtain a satisfactory outcome. Residual joint surface incongruity has been shown to cause increased local contact stress in several joints and is thought to lead to cartilage destruction when subject to repetitive forces (2,3,5,16). Secondary congruence with respect to a both-column acetabular fracture as described by Letournel is a theoretical condition that can occur in vivo by rotation of both the anterior and posterior columns around the femoral head while maintaining a congruent relationship of the head with the acetabular articular surfaces (8). This state would allow hip joint contact stresses to be more evenly distributed throughout the articular surfaces and thus result in lower peak articular contact pressures than that seen in other displaced acetabular fractures affecting the roof.

However, when compared with the unfractured acetabulum, secondary congruence is less than ideal. The hip is an incongruous joint that allows reduced contact pressures in the dome of the acetabulum by first loading its anterior and posterior portions and then plastically

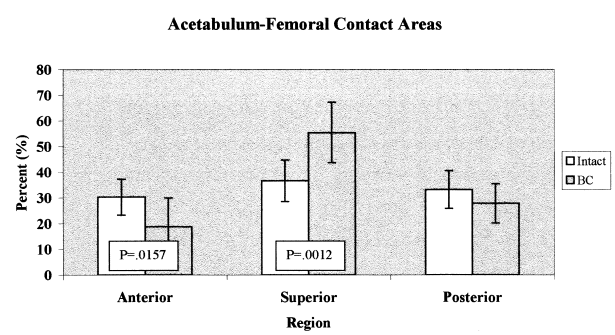

FIG. 4. Percent contact areas for the intact and both-column models. This figure indicates the percent contact areas (percent) with one standard deviation within the anterior, superior, and posterior articular regions for the intact (n = 9) and both-column (n = 9) models.

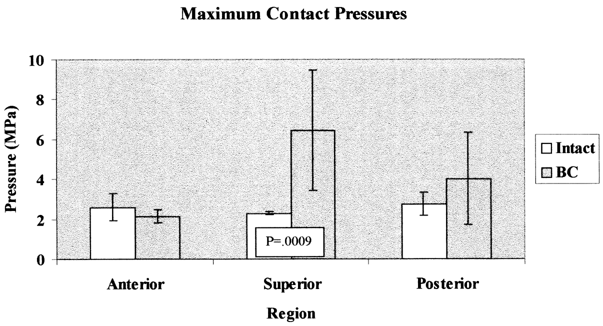

FIG. 5. Maximum contact pressures for the intact and both-column models. This figure indicates the maximum contact pressures (MPa) with one standard deviation within the anterior, superior, and posterior articular regions for the intact (n = 9) and both-column (n = 9) models.

deforming as the load is increased (1,13,14). The anterior and posterior columns rotate around the femoral head in the both-column fracture, pivoting on the labrum and capsular restraints. These structures are elastic in nature and would not be able to maintain the exact state of the unfractured acetabulum with respect to the normal deformational changes with load. Additionally, union in a position of perfect secondary congruence would create a larger acetabulum, which would likely react differently to load. The central gap created, even if it filled with fibrous tissue, would not bear stress as does articular cartilage. Intuitively, with a diminution of this deformation mechanism and reduced area in the central portion of the roof, a hip joint exhibiting secondary congruence would have increased pressures in the dome region on either side of the fracture gap. This is consistent with the data obtained in the both-column fracture model used in this study.

The results of the authors' model of secondary congruence show an increase in the contact area and mean pressure in the dome region of the acetabulum, and a decrease in these parameters in the anterior regions. The peak pressures also increased in the dome and decreased in the anterior region. The highest peak pressures were seen immediately adjacent to the fracture in all specimens.

The model used in this study was intended to simulate the in vivo conditions of a both-column acetabular fracture exhibiting secondary congruence in the healed state. The in vivo effects of bone remodeling and callus formation in the fracture gap could not be accounted for. The results obtained are specific to the model created and can be only extrapolated to the in vivo state. However, the findings of this study are similar to those of previously published reports demonstrating that consistent acetabular mechanical properties can be observed (6,14). The changes in maximum peak pressures seen in this model are in the same range as those seen in a model of transverse trans-tectal fractures reported by Olson, et al (14). However, the similarity of the biomechanical findings in these two different models does not carry over to the clinical state. Letournel reported that 11 of 13 patients treated nonoperatively for both-column fractures with good secondary congruence had good or excellent results at an average of 4.2 years (8). This is in contradistinction to the other patterns of fracture. Most other patterns of displaced fracture allow for subluxation of the head from the roof, which significantly increases the forces at the fracture site and results in poor outcomes in as many as 58 percent at one year (12).

One explanation for the similar findings in these biomechanical studies is the small amount of stepoff and gap chosen for the transverse fracture. A small displacement may not allow for subluxation of the head and might mimic more closely a both-column fracture. Letournel reported that eight of thirteen patients with fractures other than a both-column pattern had very good or good results if the head remained congruent with the roof (8). These findings have been supported by the work of Olson and Matta (12) and Tornetta (17), who reported better than 85 percent acceptable results in displaced fractures in which the head and roof were congruent.

The mild increase in mean pressure and greater increase in peak pressure found in this model are concerning. No long-term clinical study exists on the results of both-column fractures treated nonoperatively. It stands to reason that, despite these findings, the clinical success seen at three to five years justifies nonoperative management in older patients. This is further supported by the increased technical difficulty in treating fractures in osteopenic bone and because these patients, if they should fail nonoperative management, are candidates for joint-replacement surgery. The opposite is true in young patients. Joint replacement is not a good option for the young patient, so if nonoperative management fails, there is little acceptable recourse. The findings presented herein assume perfect secondary congruence of the articular surfaces of the anterior and posterior columns against the femoral head with the labrum intact as defined by a direct reduction in the cadaveric model. In the true clinical situation, perfect secondary congruence is unlikely. If the theoretical model is correct and increased loading will lead to degeneration over time, then this study supports the concept of anatomic ORIF to avoid the long-term consequences of incongruent articular loading in young patients. However, the surgeon must realize that a nonanatomic reduction may not improve the loading characteristics compared with the displaced but secondary congruent both-column fracture. Thus, a perfect reduction must be the goal if surgery is performed (11).

CONCLUSION

In the authors' both-column model of secondary congruence, the stress concentration during simulated single-leg stance was significantly increased in the dome of the acetabulum adjacent to the fracture line.

Acknowledgments: The authors would like to thank J. Russell Parsons and his laboratory staff at the University of

Medicine and Dentistry-New Jersey Medical School for their support and assistance.

REFERENCES

1. Bay B, Hamel A, Olson S, et al. Statically equivalent load and support conditions produce different hip joint contact pressures and periacetabular strains. *J Biomech* 1997;30:193–196.
2. Chrisman OD, Ledenbauer-Bellis IM, Panjabi M, et al. The relationship of mechanical trauma and the early biomechanical reactions of osteoarthritic cartilage. *Clin Orthop* 1981;161:275–284.
3. Donohue MJ, Buss D, Oegema TR, et al. The effect of indirect blunt trauma on adult canine articular cartilage. *J Bone and Joint Surg [Am]* 1983;65:948–957.
4. Heeg M, Oostvogel HJM, Klasen HJ. Conservative treatment of acetabular fractures: the role of the weightbearing dome and anatomic reduction in the ultimate results. *J Trauma* 1987;27:555–559.
5. Huber-Betzer H, Brown T, Mattheck C. Some effects of global joint morphology on local stress aberations near imprecisely reduced intra-articular fractures. *J Biomech* 1990;23:811–822.
6. Konrath GA, Hamel AJ, Sharkey NA, et al. Biomechanical evaluation of a low anterior wall fracture: correlation with the CT subchondral arc. *J Orthop Trauma* 1998;12:152–158.
7. Letournel E. Acetabular fractures: classification and management. *Clin Orthop* 1980;151:81–106.
8. Letournel E, Judet R. *Fractures of the Acetabulum, 2nd ed*. New York: Springer-Verlag, 1993.
9. Matta JM, Anderson LM, Epstein HC, et al. Fractures of the acetabulum: a retrospective analysis. *Clin Orthop* 1986;215:230–240.
10. Matta JM, Merritt PO. Displaced acetabular fractures. *Clin Orthop* 1988;230:83–97.
11. Matta JM. Fractures of the acetabulum: accuracy of reduction and clinical results in patients managed operatively within three weeks after the injury. *J Bone and Joint Surg [Am]* 1996;78:1632–1645.
12. Olson SA, Matta JM. The computerized tomography subchondral arc: a new method of assessing acetabular articular continuity after fracture (a preliminary report). *J Orthop Trauma* 1993;7:402–413.
13. Olson SA, Bay BK, Chapman MW, et al. Biomechanical consequences of fracture and repair of the posterior wall of the acetabulum. *J Bone and Joint Surg [Am]* 1995;77:1184–1192.
14. Olson SA, Bay BK, Hamel A. Biomechanics of the hip joint and the effects of fracture of the acetabulum. *Clin Orthop* 1997;339:92–104.
15. Rowe CR, Lowell JD. Prognosis of fractures of the acetabulum. *J Bone and Joint Surg [Am]* 1961;43:30–59.
16. Sangeorzan BJ, Anathakrishnan D, Tencer AF. Contact characteristics of the subtalar joint after a simulated calcaneal fracture. *J Orthop Trauma* 1995;9:251–258.
17. Tornetta III P. Nonoperative management of acetabular fractures: the use of dynamic stress views. *J Bone and Joint Surg [Br]* 1999 Jan;81(1):67–70.